Journal of Thermal Analysis, Vol. 34 (1988) 1273–1281

CHARACTERIZATION AND THERMAL INVESTIGATIONS OF AMMONIUM HEPTAMOLYBDATE

I. B. Sharma[+] and *S. Batra*

DEPARTMENT OF CHEMISTRY, UNIVERSITY OF JAMMU, JAMMU (TAWI)-180004, INDIA

(Received August 30, 1987; in revised form November 16, 1987)

Thermal decomposition of ammonium heptamolybdate was studied by means of differential scanning calorimetry and thermogravimetry. DSC showed that the material decomposes in the temperature region 463–608 K in static air atmosphere, in three steps. The products of decomposition were characterized by IR spectroscopy, elemental analysis and magnetic susceptibility measurements. All the phases are paramagnetic in nature. Kinetic analysis suggested that the first two steps are controlled by a diffusion mechanism, while the third step is controlled by nuclear-growth.

On heat treatment, ammonium heptamolybdate is reported to decompose into molybdenum oxide in three steps in the temperature region room temperature to 633 K [1, 2]. The first step, corresponding to complete dehydration, is complete at 403 K, and is followed by decomposition. The decomposition results, which are based on thermogravimetric studies, seem to be semi-quantitative. There are no data on the kinetics of the transitions. The present study is aimed at the elucidation of the precise steps of decomposition of ammonium heptamolybdate on heat treatment, determination of the kinetics of these steps and characterization of the resulting phases. The material was subjected to thermal analysis (DSC and TG–DTG) in static air atmosphere and in a continuous flow of nitrogen. IR spectra were recorded, magnetic susceptibility was measured and elemental analysis for N, H and Mo was performed to arrive at the sequence of transitions. With the program available in a TC 10 microprocessor, the kinetic parameters of the various steps involved were computed from the differential scanning calorimetric data under both dynamic and isothermal conditions. The results were analysed in light of the theory of solid-state reactions.

[+] To whom all correspondence should be addressed.

John Wiley & Sons, Limited, Chichester
Akadémiai Kiadó, Budapest

Experimental

AR grade ammonium heptamolybdate (Loba) was used as such. The elemental analysis for N, H and Mo (Table 1) suggested that the stoichiometry of the material was $(NH_4)_6Mo_7O_{24} \cdot 2H_2O$.

Ammonium heptamolybdate was thermally analysed (for DSC and TG studies) on a Mettler TA 3000 thermal analysis system, provided with a TC 10

Table 1 Analytical and physical data on the different phases drawn from the DSC cell

Temperature at which phase is drawn, K	Analysis, %			IR frequency, cm^{-1}	Molar magnetic susceptibility χ_m, cgs units × 10^6
	N	H	Mo		
Ammonium heptamolybdate	7.03	2.31	55.8	3180, 1400, 850, 690, 485, 375 and 240	925
499	5.58	1.65	60	3200, 1420, 940, 890, 730, 560, 340 and 250	898
531	3.69	1.13	62.1	3225, 1410, 945, 895, 860, 755, 625, 600–480, 430, 330 and 250	895
690	nil	nil	67	990, 880, 630, 475, 375 and 315	910

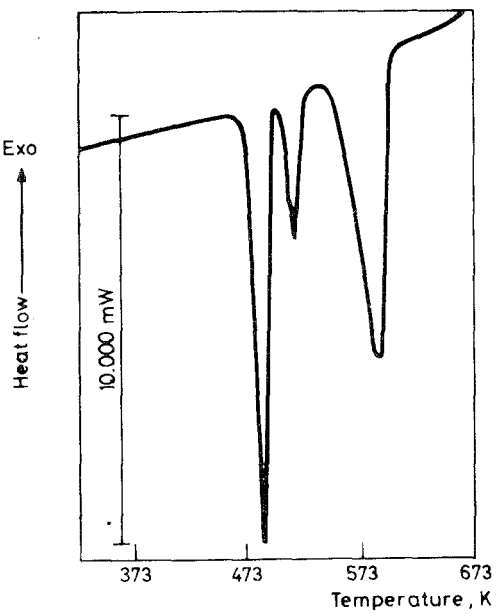

Fig. 1 The DSC curve (dH/dt *vs.* T) for ammonium heptamolybdate at the heating rate of 10 deg/min in static air atmosphere

microprocessor, in static air atmosphere and in a continuous flow of nitrogen (30 ml/min). The DSC (dH/dt *vs.* T) and TG–DTG curves, recorded in static air atmosphere at a heating rate of 10 deg/min, are given in Figs 1 and 2, respectively. The kinetic parameters computed from the DSC data and the TG results are given in Table 2. The isothermal data (fraction of reaction completed vs. time) were recorded at different temperatures for the different transitions. The data are shown in Figs 3–5.

IR spectra

The IR spectra of ammonium heptamolybdate and the samples drawn from the DSC cell after runs up to 499, 531 and 690 K in static air atmosphere were recorded on a Pye Unicam SP 2000 spectrophotometer. The data are given in Table 1. The IR spectra for the samples drawn in static air atmosphere and in nitrogen atmosphere display complete similarity.

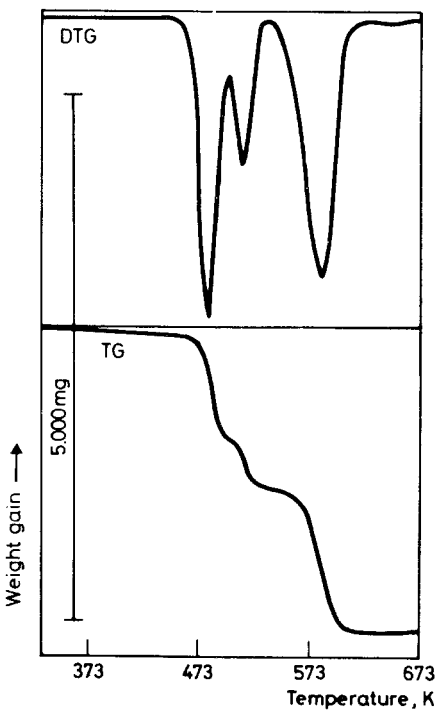

Fig. 2 The TG–DTG curves for ammonium heptamolybdate at the heating rate of 10 deg/min in static air atmosphere

Table 2 Kinetic data on thermal decompositions of ammonium heptamolybdate in static air atmosphere

Transition temperature, K DSC/TG	Peak temperature, K DSC/TG	n	E, kJ/mole	ln A	H, kJ/mole	Mass loss, %
463–498/445.3–498.7	483.1/480	1.35	641	156	236	5.42
498–528/498–530.7	515.1/509	1.41	693	159	70	2.40
543–608/530.7–685.3	586.6/584.1	0.74	244	45	368	7.83
	In continuous flow of nitrogen					
465.7–503/474.2–537.7	484.7/517	1.42	840	206	229	5.37
503–533/537.7–567.4	517.6/549.1	1.69	910	208	76	2.46
537–619/567.4–687	601.4/613.2	1.05	226	41	382	7.44

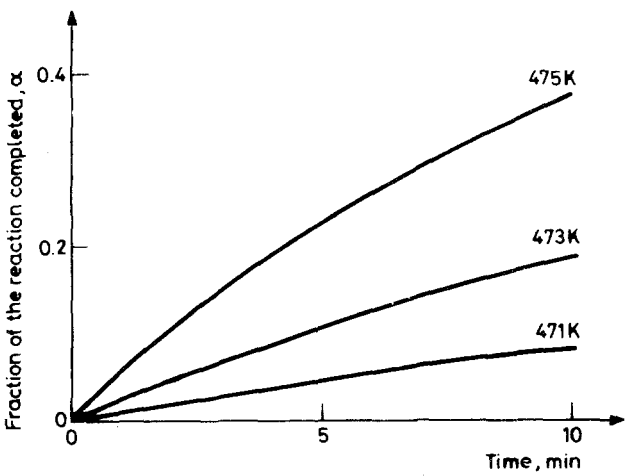

Fig. 3 α versus t from the differential scanning calorimetry for the first step of decomposition

Elemental analysis

The samples drawn from the DSC cell after heat treatment up to 499, 531 and 690 K in static air atmosphere were analysed for nitrogen and hydrogen with a Carlo Erba 1106 elemental micro-analyser. Different samples drawn at various stages of decomposition were analysed for molybdenum by the usual methods. The results are given in Table 1.

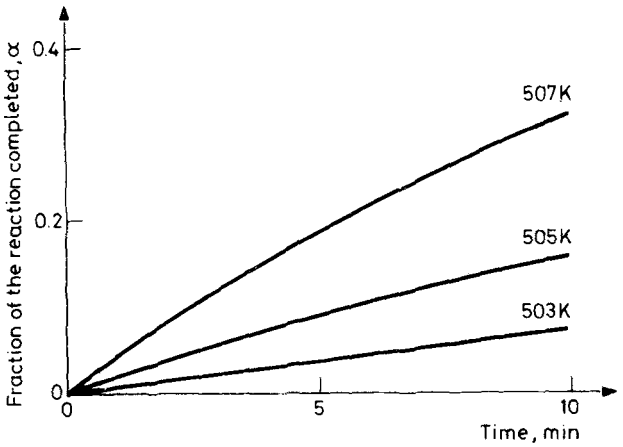

Fig. 4 α *vs.* t from the differential scanning calorimetry for the second step of decomposition

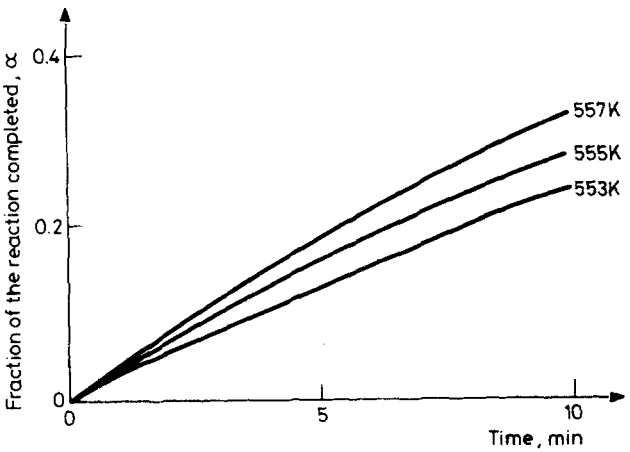

Fig. 5 α *vs.* t from the differential scanning calorimetry for the third step of decomposition

Magnetic susceptibility

The room-temperature magnetic susceptibilities of the samples used for elemental analyses were measured with a Gouy magnetic balance, using $HgCo(CNS)_4$ as calibrant. The field strength was kept constant at 3000 gauss for all measurements. The magnetic susceptibility associated with each sample, after diamagnetic correction for the constituent ions, is given in Table 1.

Results and discussion

The differential scanning calorimetric curve for $(NH_4)_6Mo_7O_{24}\cdot 2H_2O$ at a scanning speed of 10 deg/min (Fig. 1) exhibits three endothermic transitions, in the temperature regions 463–498, 498–528 and 543–608 K, with peak temperatures at 483.1, 515.1 and 586.6 K, respectively. The DSC data measured in the nitrogen atmosphere show the same three endothermic transitions, with the transition temperatures slightly shifted (Table 2).

The TG–DTG curve recorded in static air atmosphere (Fig. 2) exhibits three mass loss steps, in the temperature regions 445.3–498.7, 498.7–530.7 and 530.7–585.3 K, with mass losses of 5.42, 2.40 and 7.83%, respectively. The mass loss data measured in nitrogen (Table 2) show the corresponding three steps. However, the temperature regions were shifted to higher temperature, as observed in the DSC case, and the corresponding mass losses were slightly different (5.37, 2.46 and 7.44%, respectively).

The mass loss data from TG in static air atmosphere (Table 2) and the elemental analysis for N, H and Mo for the sample drawn after the three mass loss steps suggest the following decomposition sequence for $((NH_4)_2O)_37MoO_3\cdot 2H_2O$ on heat treatment:

$$((NH_4)_2O)_37MoO_3\cdot 2H_2O \xrightarrow{445.3\text{–}498.7\ K} ((NH_4)_2O)_{2.4}7MoO_3$$

$$\xrightarrow{498.7\text{–}530.7\ K} ((NH_4)_2O)_{1.7}7MoO_3 \xrightarrow{530.7\text{–}685.3\ K} 7MoO_3$$

There is a simultaneous loss of the water molecules and of $(NH_4)_2O$ in the first step. The next two transitions are accompanied by deammoniation. The data from the thermogravimetric curve measured in a continuous flow of nitrogen indicate that the transition temperatures are slightly shifted to higher values.

The IR data for the different samples are given in Table 1. The broad band in the region 3600–2400 cm^{-1} for the original sample is attributed to the presence of the NH_4^+ group and the O—H stretching vibration of water [3]. The band is broadened due to the overlap of the two different vibrations in the same region. The much sharper band for the next two samples is due only to the NH_4^+ group. This is not present in the spectrum of the final product. The peak in the region 520–460 cm^{-1} for the original sample, which is attributed to the vibrational mode of the water molecule, demonstrates the presence of water in the sample. No such peak is observed in the spectra of the remaining samples. The band at around 1400 cm^{-1} for the first three samples is due to the NH_4^+ group. The broad peaks observed in the regions 700–500 cm^{-1} and 1050–810 cm^{-1} in the spectra of all the samples are

attributed to metal-oxygen bonds. The IR data suggest that ammonium heptamolybdate is originally associated with water molecules, while all the samples except the final product have NH_4^+ groups present in them. This is in accordance with the scheme postulated above for the transitions.

The literature thermal data [1] suggest that ammonium heptamolybdate tetrahydrate is completely dehydrated at 403 K. However, the present study shows no such transition, in either TG or DSC, in this temperature region. The present study demonstrates that the dehydration accompanied by the deammoniation process starts at 463 K in the DSC, while the TG results suggest initiation of this process at 445.3 K. The remaining $(NH_4)_2O$ is lost in the next two steps. This process is facilitated in static air atmosphere, while in a continuous flow of nitrogen the decomposition steps are complete at slightly higher temperatures. The thermogravimetric data show that the decomposition process is complete at 685.3 K in static air atmosphere.

Kinetic analysis

The kinetic parameters were calculated from the DSC data via the equation [4, 5]:

$$\frac{d\alpha}{dt} = A\, e^{-E/RT}(1-\alpha)^n$$

where α is the fraction of the reaction completed in time t, n is the order of the reaction, E is the energy of activation and A is the frequency factor.

If it is assumed that the fraction of the reaction completed is proportional to the DSC signal, the above equation can be transformed to the following logarithmic form:

$$\frac{\ln dH/dt}{H_t} = \ln A + n \ln H_r/H_t - E/RT$$

where dH/dt is the heat flow in mW, H_t is the total enthalpy of the reaction (total area of the peak) and H_r is the remaining area of the DSC peak. Since dH/dt, H_t, H_r and T are known, other parameters (n, A and E) can be calculated with the help of the TC 10 microprocessor provided with the TA 3000 thermal analysis system. The computed values of n, $\ln A$ and E for the different transitions in static air atmosphere are given in Table 2. The values of the energy of activation and the frequency factor for the first two transitions are high and of the same order. The similarity suggests that the mechanisms involved may be similar, while the elevated values suggest the simultaneous breaking of a number of bonds and a highly disordered activated state. However, the values of E and $\ln A$ are comparatively low in the third transition, which suggests that a different mechanism is involved in the

process. Comparison of the kinetic parameters in nitrogen and static air atmosphere (Table 2) suggests that the corresponding mechanism remains unaltered in each case.

For elucidation of the mechanism of the reactions involved, various kinetic equations applicable to solid-state reactions were applied to the isothermal data from differential scanning calorimetry (Figs 3–5). It was observed that the data for the first two transitions follow the Ginstling–Brounshtein equation for diffusion-controlled reactions [6]. Plots of $(1-2/3\alpha-(1-\alpha)^{2/3})$ *vs.* t gave straight lines in both cases. For the data on the third transition, the Avrami–Erofeev equation for a nuclear growth mechanism in the form $kt = -\ln(1-\alpha)^{2/3}$ is applicable [7, 8]. These results suggest that the first two transitions are governed by a diffusion process where the reaction surface for spherical particles decreases in area as the reaction proceeds. In the last transition, which is controlled by a nuclear growth process, a product phase with different shapes is formed from a constant number of nuclei in a matrix of different compositions.

* * *

The authors are grateful to the UGC, New Delhi, for financial assistance.

Reference

1 E. Ma, Bull. Chem. Soc. Japan, 37 (1964) 171.
2 J. C. Bailer, H. J. Emeleus, R. Nyholm and A. F. T. Dickenson, Comprehensive Inorganic Chemistry, Vol. 3, Pergamon, Oxford 1973, p. 735.
3 K. Nakamoto, Infrared Spectra of Inorganic and Coordination Compounds, Wiley, New York, 1963, pp. 72, 83, 104.
4 P. Peyser and W. D. Bascom, Analytical Calorimetry, Vol. 3, eds. R. S. Porter and J. F. Johnson, Plenum, New York 1974, p. 537.
5 I. B. Sharma and S. Batra, Indian J. Chem., 26A (1987) 736.
6 A. M. Ginstling and B. T. Brounshtein, J. Appl. Chem., USSR (English Transl.), 23 (1950) 1327.
7 M. Avrami, J. Chem. Phys., 9 (1941) 177.
8 B. V. Erofeev, Cr. Acad. Sci. USSR, 52 (1946) 511.

Zusammenfassung — Mittels Differential-Scanning-Kalorimetrie und Thermogravimetrie wurde die thermische Zersetzung von Ammoniumheptamolybdat untersucht. Laut DSC zersetzt sich die Substanz in statischer Luftatmosphäre im Temperaturbereich von 463 bis 608 K in drei Schritten. Die Produkte wurden durch IR-Spektroskopie, Elementaranalyse und Messungen der magnetischen Suszeptibilität charakterisiert. Alle Phasen sind paramagnetischer Natur. Kinetische Untersuchungen besagen für die ersten zwei Schritte einen diffusionskontrollierten, für den dritten Schritt einen wachstumskontrollierten Mechanismus.

Резюме — С помощью дифференциальной сканирующей калориметрии и термогравиметрии изучено термическое разложение гептамодибдата аммония. Результаты ДСК показали, что вещество в статической атмосфере воздуха разлагается в температурном интервале 463–608 К в три стадии. Продукты разложения были охарактеризованы ИК спектрами, элементным анализом и измерениями магнитной восприимчивости. Все образующиеся при этом фазы являлись парамагнитными. Кинетический анализ показал, что первые две стадии контролируются диффузионным механизмом, тогда как третья стадия — ростом центров кристаллизации.